European Conference on Computational Fluid Dynamics
ECCOMAS CFD 2006
P. Wesseling, E. Oñate, J. Périaux (Eds)

SHAPE OPTIMIZATION OF AXISYMMETRIC EJECTOR

V. Dvořák*

*Technical University of Liberec, Faculty of Mechanical Engineering,
Department of Power Engineering Equipment
Hálkova 6, 46117 Liberec 1, Czech Republic
e-mail: vaclav.dvorak@tul.cz
Web page: http://www.kez.tul.cz/

Key words: Ejector, Mixing process, Shape optimization, Dynamic mesh.

Abstract: *This contribution deals with aerodynamic optimization using dynamic mesh method provided by Fluent software. A method of transformation of coordinates and an optimization procedure enabling to obtain arbitrary shape of computing mesh are described. This method was developed for shape optimization of axisymmetric ejector in order to obtain the highest efficiency of the whole device. A result of using this method is a series of ejector shapes for different relative back pressure values. Resulting values of efficiency of optimized ejectors, optimal area ratios, optimal ejection ratios and velocity ratios are presented. An analysis of mixing in optimized ejector is carried out.*

1 INTRODUCTION

This contribution deals with aerodynamic optimization using dynamic mesh method provided by Fluent software. So we continue in work[1], in which the shape optimization of the mixing chamber and of the diffuser of axisymmetric ejector was solved. A series of optimized shapes of the ejector for different values of relative back pressure Π was the result of these calculations. The resulting efficiencies were better than in case of a simple ejector with constant area mixing chamber and with conic diffuser[2]. The computing mesh was deformed only in radial direction. That did not allow to form arbitrarily the inlet part of the ejector, which was then kept constant, as we can see in Fig. 1a. The inlet area ratio of cross-sections of nozzles $\mu = A_1/A_2$ was than kept constant too. It is obvious that chosen ratio $\mu = 0.3$ is optimal only for certain relative back pressure ($\Pi \approx 0.25$ see Fig. 1c), while it is unsuitable for different back pressure. It is the reason why the shapes of the entrance part of the mixing chamber are unnatural for extreme values of back pressure (see Fig. 1b for $\Pi = 0.1$ and Fig. 1d for $\Pi = 0.5$). The development of a method enabling a complex optimization of the ejector including its inlet part was the objective of the next work[3]. It made the determination of the optimal inlet area ratio μ for given back pressure possible. It is obvious from Fig. 2 that this method enables deformation of computing mesh both in radial direction - y and axial direction - x.

2 METHODS

Fluent 6.1 software, which provides several method of dynamic mesh, was used for computation. We used a method enabling direct setup of positions of each node of the computational domain - user defined deforming. The advantage of using dynamic mesh for optimization consists in reduction of computing time. It does not need to initialize each new variant of the computing mesh shape. The solution from past time step of the past mesh is only recalculated. The reduction of the computing time is all the more important, because we need an entirely converged solution to evaluate the objective function and to compare two variants of solution properly. The shape similarity of the computing meshes for individual variants of the solution is the next advantage of using dynamic mesh.

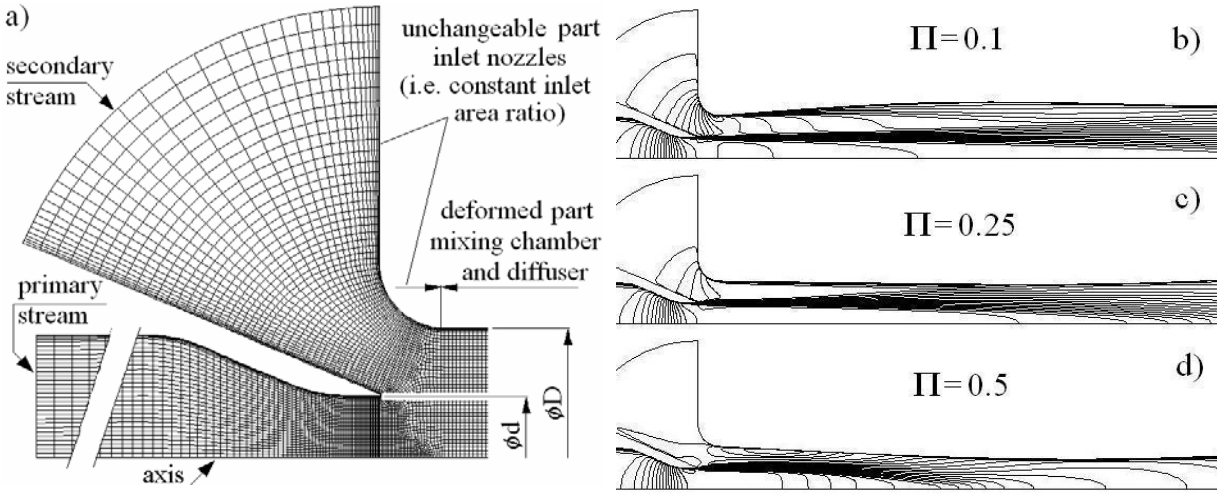

Fig. 1: a – ordering of computing mesh for optimization of the mixing chamber and diffuser of the ejector with constant inlet area ratio[1]. Velocity contours in resulting shapes of the ejector for different values of relative back pressure: b - $\Pi = 0.1$ - inlet area ratio μ is too small, c - $\Pi = 0.25$ - μ is just about optimum, d - $\Pi = 0.5$ - μ is too big[1].

2.1 Dynamic mesh and optimization procedure

Method used for deformation of computing mesh is in Fig. 2. The cartesian coordinate system $[x, y]$ was replaced by coordinate system $[\xi, \zeta]$. The independent coordinate ξ represents the length of the control curve from its beginning in the point $[x_0, y_0]$, whereas dependent coordinate ζ represents displacement from the control curve in the direction perpendicular to the control curve. The optimization procedure then deals only with finding of optimal displacement ζ of chosen points on the wall of the ejector. The resulting shape of the ejector is then given by normal cubic spline function constructed in $[\xi, \zeta]$ coordinate system through control points. The displacement of individual nodes of the computing mesh depends on relative distance ψ. Nodes on the fixed axis and nodes adjacent to the fixed mesh have $\psi = 0$, nodes on deformed wall including control points have $\psi = 1$.

An easy optimization algorithm was used for finding of optimal displacement of wall points. Value of displacement ζ_j of only one point j was changed in each optimization step. Then the next first point downstream followed. About 1000 time steps were necessary to get an optimal shape. The method is more detailed described in[3].

The objective function for optimization of the ejector is total efficiency η, which is given by relation for compressible flow. Because the whole optimization runs with constant setup of boundary conditions, the objective function is then ratio of mass flow rates, the ejection ratio[4]

$$\Gamma = m_2 / m_1 \,. \tag{1}$$

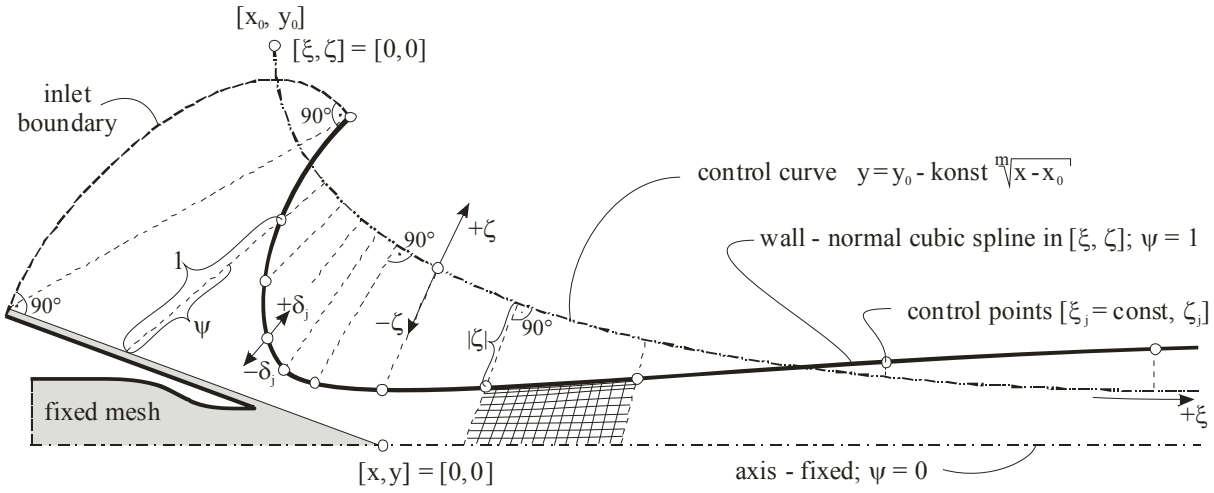

Fig. 2: Transformation of coordinate system and deformation of computing mesh.

2.2 Numerical model

The segregated solver was used to provide faster convergence, the flow was considered to be compressible. Turbulence model was k-ε realizable, which is suitable for computation of axi-symmetric ejector[2]. The calculation mesh and setup of the boundary condition are obvious from Fig. 3. The computation domain is divided into two parts. First part is the fixed unchangeable part and consists mainly of the nozzle of the primary stream. Second part is optimized and during the procedure will form the inlet of secondary stream, the mixing chamber and the diffuser. The initial values ξ, ψ of each node and initial values ξ_j, ζ_j, δ_j of control points were adjust in the first time step.

Boundary conditions were chosen as: pressure inlet p_{01} for primary stream, p_{02} for secondary stream and pressure outlet p_b for the outlet from the ejector, as we can see in Fig. 3. The relative back pressure is then given by the ratio

$$\Pi = \frac{p_b - p_{02}}{p_{01} - p_{02}} \,. \tag{2}$$

The boundary condition of secondary flow is changed during optimization to ensure that it

is perpendicular to the walls, as we can see in Fig. 3. The inside diameter of the primary nozzle is $d = 19.2$ mm.

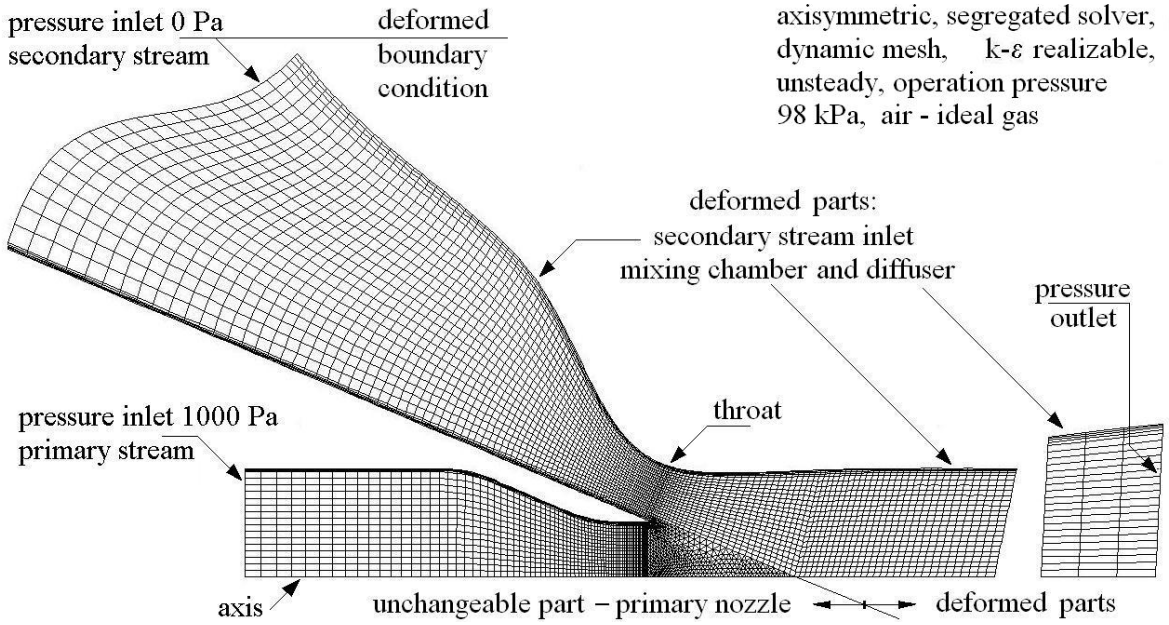

Fig. 3: Computing mesh and setup of boundary conditions.

3 RESULTS AND DISCUSSION

It was found out during the optimization that the formation of backward diverging part of the ejector – diffuser and also the formation of inlet area ratio μ have dominant influence on the development of the objective function. The inlet part - the inlet of the secondary stream - is not so important for the resulting ejector efficiency. The shape of the inlet part was expected to be similar to the shape in Fig. 1 and hence it was initialized in this way. The formation of the inlet part occurred after final optimization of the mixing chamber and diffuser. The formation ended similarly to the Fig. 4b with the wide inlet part in some cases. The inlet part was formed into the narrowed variation another time, see Fig. 4a, 4c and 4d. The narrowed variation gives higher efficiency as was proved during repeating optimization of wider cases. The difference of the objective function was about 0.5 percent. The narrow inlet part was reached for back pressure values $\Pi = 0.1$ and $\Pi = 0.2$, but not for $\Pi = 0.15$. It can indicate that the objective function has two local maximums and used method is not able to find the higher one. A question remains: how the deformation and extension of computing faces in inlet boundary condition near the ejector wall influence the objective function for wider variation of the inlet part – see Fig. 4b for $\Pi = 0.15$. The inlet part has a gently slope from the beginning and just in front of the entrance to the mixing chamber and formation of the ejector throat is the slope steeper for middle values of back pressure $\Pi = 0.2 \div 0.35$. The inlet part is wide and similar to the one from Fig. 1 for high back pressures $\Pi = 0.4 \div 0.5$.

This all could confirm that the ambiguity of the shape of the inlet part is caused by deformation – extension – of computing faces in inlet boundary condition near the ejector wall – in the boundary layer. The inlet velocity of the secondary flow is higher for low back pressures and influence of deformed boundary layer more expressive, so that the narrow inlet is formed. The influence of boundary layer faces could be negligible for high back pressure with low inlet velocity of secondary flow – see Fig. 4e for $\Pi = 0.4$ and Fig. 4f for $\Pi = 0.5$.

The optimization was made for ten values of relative back pressure from $\Pi = 0.05$ to $\Pi = 0.5$. We focus mainly on the results obtained for $\Pi = 0.25$.

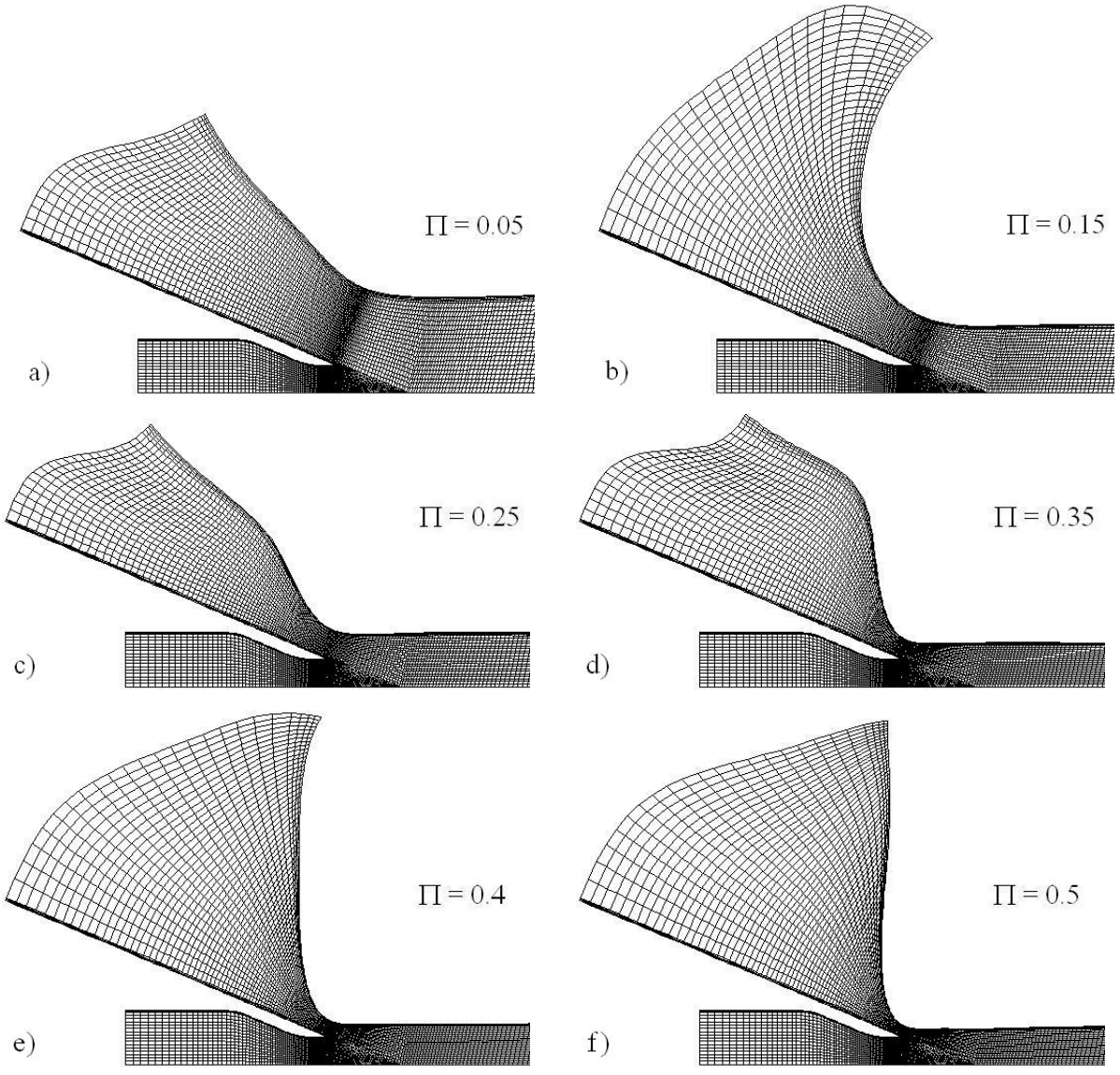

Fig. 4: Resulting shapes of computing mesh in the inlet parts for various back pressure.

There are contours of velocity magnitude and of static pressure in the ejector optimized for relative back pressure $\Pi = 0.25$ in Fig. 5. Final shape of the ejector results in a smooth connection between the individual parts of the ejector – the inlet part including inlet of secondary stream, the mixing chamber and the diffuser. The narrowest cross section, the first throat of the ejector, is just behind the trailing edge of the primary stream nozzle, where both flows meet. After the consequent slow enlargement of the mixing chamber a next necking follows which forms second throat of the ejector. Then the mixing chamber extends again and slowly passes into the diffuser.

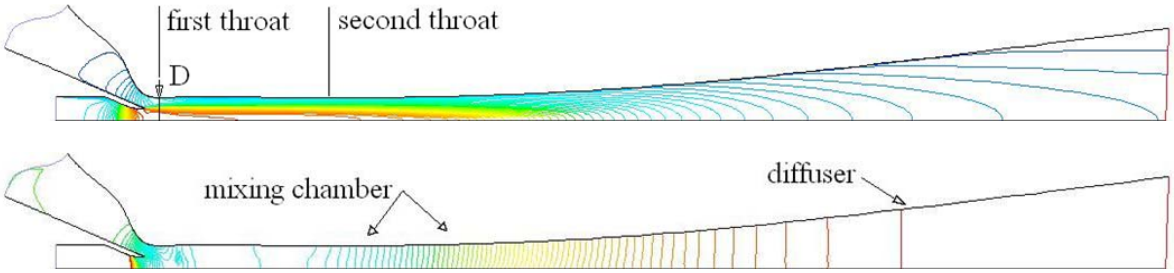

Fig. 5: Contours of velocity magnitude and of static pressure in the ejector optimized for $\Pi = 0.25$.

The values of resulting efficiencies η for ejector optimized by described method are presented in Fig. 6a. We can see that the maximal efficiency is achieved for relative back pressure approximately $\Pi = 0.2 \div 0.3$, when the level of 30 percent was reached. The efficiency is lower for different back pressure, but even for high back pressure $\Pi = 0.5$ the efficiency is still 25 percent. A rapid drop of the efficiency for $\Pi = 0.05$ could be caused by the limited length of the model ejector. For the low back pressures, the mixing chamber and the whole ejector are bigger and therefore the length of the model ejector is insufficient. In Fig. 7 are also presented efficiencies of ejector with $\mu = 0.3$ and with optimized mixing chamber[1] and efficiencies of simple ejector according to reference[2]. We can see that for $\Pi > 0.35$ the efficiency of the simple ejector is negative, because the mass flow rate of the secondary stream m_2 is negative too. All presented results were obtained while using turbulence model k-ε realizable.

The resulting values of objective function – ejection ratio Γ in dependence on relative back pressure Π are presented in Fig. 6b. We can see that the value of Γ and also the value of inlet area ratio μ decrease with increase of back pressure. Values of inlet velocity ratio $\omega = v_2/v_1$ are carried out in Fig. 6b too. The ratio of velocities in the first throat of the ejector – the inlet velocity ratio - is calculated by relation

$$\Gamma = \frac{m_2}{m_1} = \frac{A_2 v_2 \rho_2}{A_1 v_1 \rho_1} = \frac{\omega}{\mu} \frac{\rho_2}{\rho_1}, \tag{3}$$

where ρ_1 is density of primary stream and ρ_2 density of secondary stream.

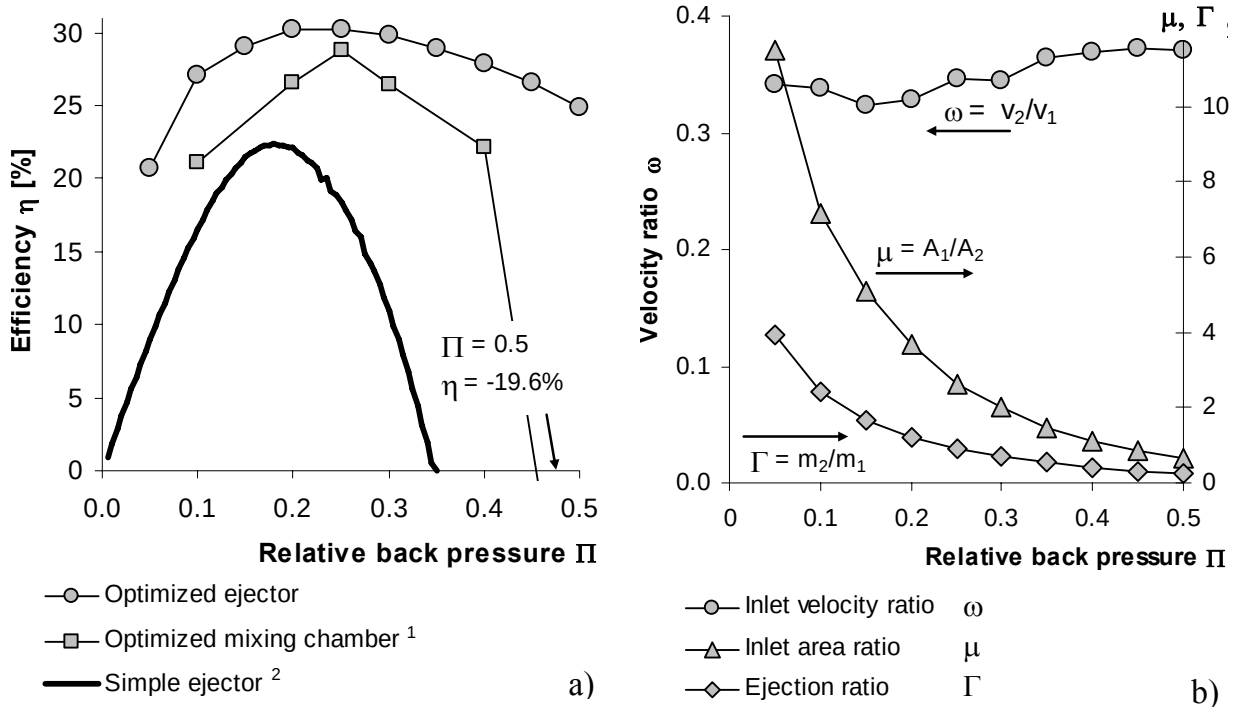

Fig. 6: a - comparison of achieved efficiencies of optimized ejector, of the ejector with constant inlet area ratio and with optimized mixing chamber and diffuser[1] and of the simple ejector with constant area mixing chamber and conic diffuser[2]; b – resulting values of ejection ratio, inlet area ratio and inlet velocity ratio ω.

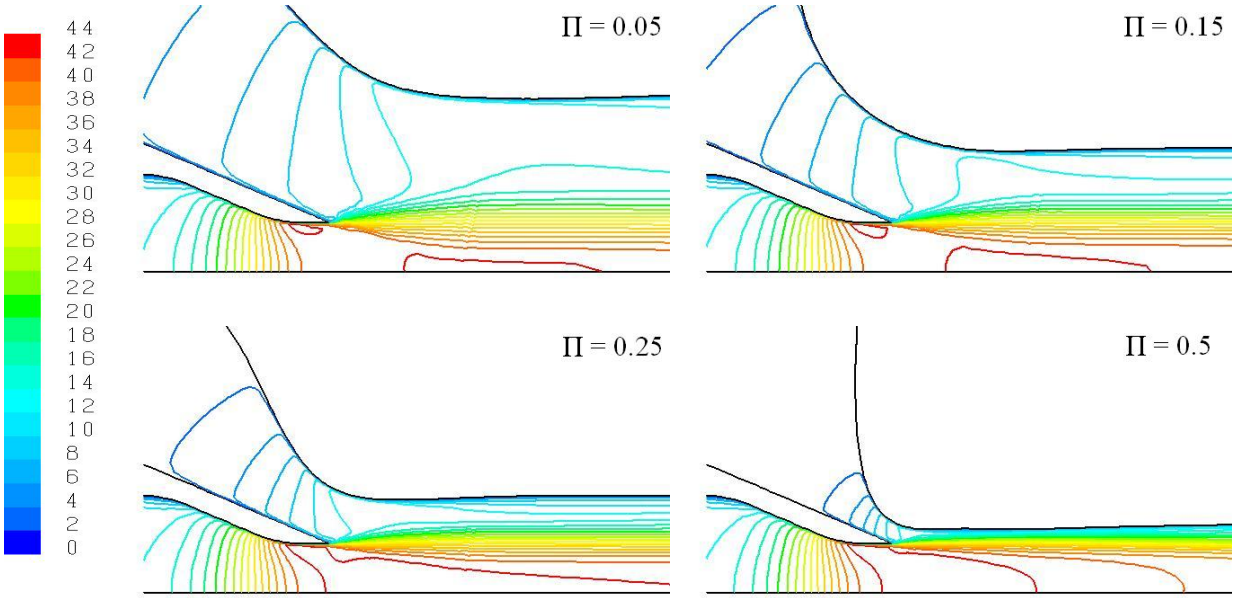

Fig. 7: Contours of velocity magnitude in the entrance part of the mixing chamber for various back pressure.

We can see that the values of the optimal inlet velocity ratio are almost independent on the back pressure. The optimal velocity ratio tends to grow with increase of the back pressure. It can be in connection with frictional losses in the mixing chamber. The ejector is shorter and frictional losses smaller for the higher back pressure. Smaller losses then yields higher velocity ratio. Contours of velocity magnitude in the entrance part of the mixing chamber for chosen back pressures are presented in Fig. 7. We can also see the narrowest part of the ejector – the first throat – which defines the inlet area ratio according to the relation

$$\mu = \frac{A_1}{A_2} = \frac{d^2}{D^2 - d^2}. \tag{4}$$

The static pressure distribution on the walls of ejectors for various relative back pressure are presented in Fig. 8. The curves seem to be similar. The pressure drops at the beginning to the level of -140 Pa just behind the trailing edge of the nozzle. This pressure drop is caused by overexpansion of the secondary stream on the curved ejector throat. A small pressure increase and region of approximately constant pressure of -90 Pa follows. This region is very short for high back pressure and long for low back pressure. This region matches to the initial region of mixing according to the theory by Tyler and Williamson[5]. The initial region is a place, where the shear layer does not reach the wall of the mixing chamber and so that the primary stream forms a free jet[6]. The main region of the mixing begins just behind the initial region. The shear layer spreads across of the whole mixing chamber and the static pressure increases very intensively in the main region of mixing.

Static pressure distribution on the wall of the ejector optimized for $\Pi = 0.25$, contours of velocity magnitude and development of momentum coefficient are presented in Fig. 9. The momentum coefficient β is defined by the ratio

$$\beta = \frac{A\int v^2 dA}{(\int v dA)^2}, \tag{5}$$

which describes misalignment of the velocity profile. We can see that the momentum coefficient has its maximum in the beginning of mixing and then drops. The loss of the momentum coefficient is more intensive in the initial region of mixing than it is in the main region of mixing. That contrasts with constant area mixing, where the loss of the momentum coefficient is slow in the initial region, whereas drops rapidly in the main region to the value of fully developed turbulent flow $\beta \cong 1.02$. Faster falling of the momentum coefficient can be caused by narrowing of the mixing chamber in the initial region, whereas the mixing chamber expands in the main region. The minimum of the momentum coefficient is $\beta_{\min} \cong 1.06$ and can define the transition between the mixing chamber and the diffuser. The deceleration of the flow yields increase of the momentum coefficient in the diffuser. The static pressure rise is mainly realized in the main region of mixing. A part of this pressure growth is nearly linear. The rest of the pressure growth in the diffuser is insignificant.

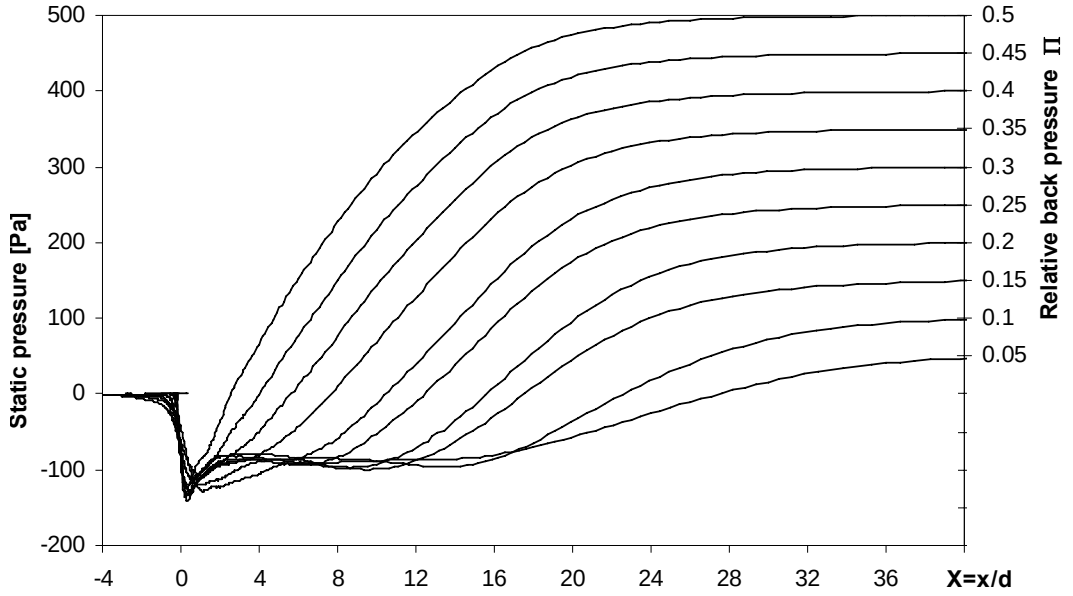

Fig. 8: Static pressure distribution on the walls of optimized ejectors.

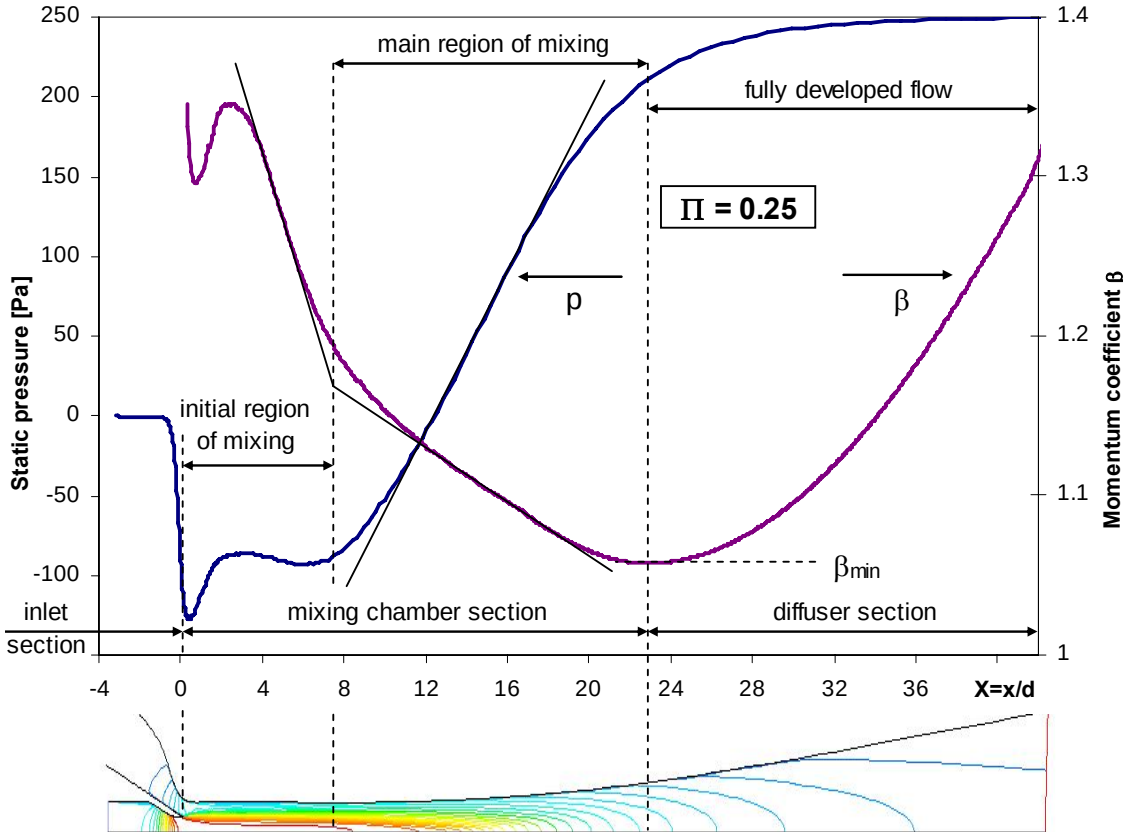

Fig. 9: Static pressure distribution on the wall, curve of momentum coefficient and contours of velocity magnitude of the ejector optimized for $\Pi = 0.25$.

4 CONCLUSION

A method of aerodynamic optimization using dynamic mesh was developed. This method was used for the shape optimization of the inlet part, of the mixing chamber and of the diffuser of the ejector. Axisymmetric ejector was optimized for different values of relative back pressure. Optimal values of the inlet area ratios and of the ejection ratios were calculated. It was found out that the optimal value of the velocity ratio is nearly independent on the back pressure. The momentum coefficient has its minimum in the end of mixing and this place was suggested to be a transition between the mixing chamber and the diffuser. The major growth of the static pressure is realized in the main region of mixing in the mixing chamber.

It is necessary to improve the method of deforming of the computing mesh to prevent the pulling of the faces of the boundary layer and to ensure obtaining of unique results of the shape of the inlet part. It is also necessary to use resulting shapes of the ejector for initialization of the mesh of higher density to model the mixing more accurately. It will be also helpful to include the shape of the primary stream nozzle into the optimization and to analyze the results. We should keep in mind that the results are obtained numerically and they will have to be experimentally verified.

Acknowledgments

This project was realized with financial support from the state resources by the Czech Science Foundation, grant no. 101/05/P298 "Optimization and control of mixing processes" and with financial support from MSM 4674788501.

REFERENCES

[1] Dvořák V.: “Shape optimization of ejector mixing chamber”, *Colloquium Fluid Dynamics*, Institute of Thermomechanics AC CR, 19. - 21. 10. 2005, pp. 29 - 32, Prague, Czech Republic, 2005.

[2] Dvořák V., Vít T.: “Experimental and Numerical Study of Constant Area Mixing”, *16th International Symposium on Transport Phenomena*, 29. 8. - 1. 9. 2005, Prague, Czech Republic.

[3] Dvořák V.: “Use of dynamic mesh for shape optimization of ejectors”, *Proceedings of the 12th conference of Fluent users*, June 7 – 9, 2006, Hrotovice, Czech Republic (in print).

[4] El-banna R.A.M.: *An investigation of New Concepts in Twodimensional Curved Thrust Augmentors*. Ph.D. thesis 1983 - 1986, supervisor Adkins R.C., Cranfield Institution of Technology, Schooll of Mechanical Engineering, Great Britain 1986.

[5] Tyler, R. A., Williamson, R. G.: *Confined mixing of coaxial flows*. Aeronautical report LR-602, NRC no. 18831, Division of Mechanical Engineering, Ottawa, Canada 1980.

[6] Dvořák V., Fridrich J.: “Experimental and numerical verification of analytical method of computation of constant area mixing”, *Topical Problems of Fluid Mechanics*, IT ASCR, February 17 - 18, 2006, pp. 31 - 34, Prague, Czech Republic, 2006.